INITIAL AERODYNAMIC AND ACOUSTIC STUDY OF AN ACTIVE TWIST ROTOR USING A LOOSELY COUPLED CFD/CSD METHOD

D. Douglas Boyd, Jr.
Research Aerospace Engineer, Aeroacoustics Branch
NASA Langley Research Center
Hampton, Virginia, USA 23681-2199
David.D.Boyd@nasa.gov

35th European Rotorcraft Forum
September 22-25, 2009
Hamburg, Germany

ABSTRACT

Preliminary aerodynamic and performance predictions for an active twist rotor for a HART-II type of configuration are performed using a computational fluid dynamics (CFD) code, OVERFLOW2, and a computational structural dynamics (CSD) code, CAMRAD-II. These codes are loosely coupled to compute a consistent set of aerodynamics and elastic blade motions. Resultant aerodynamic and blade motion data are then used in the Ffowcs-Williams Hawkins solver, PSU-WOPWOP, to compute noise on an observer plane under the rotor. Active twist of the rotor blade is achieved in CAMRAD-II by application of a periodic torsional moment couple (of equal and opposite sign) at the blade root and tip at a specified frequency and amplitude. To provide confidence in these particular active twist predictions for which no measured data is available, the rotor system geometry and computational set up examined here are identical to that used in a previous successful Higher Harmonic Control (HHC) computational study. For a single frequency equal to three times the blade passage frequency (3P), active twist is applied across a range of control phase angles at two different amplitudes. Predicted results indicate that there are control phase angles where the maximum mid-frequency noise level and the 4P non-rotating hub vibrations can be reduced, potentially, both at the same time. However, these calculated reductions are predicted to come with a performance penalty in the form of a reduction in rotor lift-to-drag ratio due to an increase in rotor profile power.

1. INTRODUCTION

Rotorcraft noise has been a subject of intense research in both the civilian and military communities for several decades. Research and understanding of rotorcraft noise issues aid in the ability to meet noise certification of civilian rotorcraft and the ability to improve the survivability of a military rotorcraft. Under the NASA Fundamental Aeronautics Program (FAP), the Subsonic Rotary Wing Project (SRW) has as a set of goals the development of rotorcraft noise prediction and measurement capabilities. The prediction efforts aim to develop “first principles” methods using coupled computational fluid dynamics (CFD), computational structural dynamics (CSD), and acoustic prediction methods. SRW also has as a goal to examine active rotor concepts that have the potential to control rotor vibrations, noise, etc.

In the past, a number of different active rotor control strategies have been examined experimentally and computationally by various organizations. Extensive discussion of some of these active rotor concepts for Blade Vortex Interaction (BVI) noise can be found in Reference 1. Some of the technologies discussed are Higher Harmonic Control (HHC) of blade pitch motion through manipulation of the swashplate motion and Individual Blade Control (IBC) of blade pitch using hydraulic pitch link actuators and embedded distributed actuators along the blade span to twist the rotor blade. Only the prediction of active twist will be examined in the current study.

In line with the NASA goals under the SRW Project, the present effort provides initial preliminary aerodynamic, acoustic, and performance predictions for a subset of possible cases for a possible future international collaborative active twist rotor test, which is in the initial planning stages. This potential test is expected to involve a HART-II like configuration and experiment in the DNW. Because there are no experimental results for an active twist rotor for this particular configuration, the following sections discuss how the predictions are framed – and some of the history behind these predictions – in order to provide a high level of confidence in the computed results.

1.1 Higher Harmonic Control (HHC)

The use of HHC active control technique can be observed in a test conducted in 2001. This test, known HART-II [Ref. 2], was conducted in the large German-Dutch Wind Tunnel (DNW) low-speed facility (LLF). This experiment was of a 40% scale

BO-105 model rotor and examined the effects of HHC of rotor blade pitch on noise and vibration. The main emphasis of the test was a descent flight condition where blade-vortex interaction (BVI) is dominant. Several of the HART-II cases have been extensively examined with numerical methods. In the United States, some of the non-CFD noise prediction methods for these cases have been based on high resolution comprehensive analysis. For example, the CAMRAD.Mod1 / HIRES / WOPWOP [Ref. 3] code suite was developed in the early and mid-1990s as a tool for harmonic and BVI noise prediction. While this model and its successors [Ref. 4, 5] provided good correlations with HART-like configurations, it was not a first principles analysis and still relies on some empiricism and assumptions. First principles, CFD-based loosely coupled predictions on the HART-II configuration using OVERFLOW2 [Ref. 6] and CAMRAD-II [Ref. 7] were first performed by Lim, et al [Ref 8]. Subsequent noise predictions in Reference 9 used compact chordwise blade loading and rigid blade motion based on predictions from Reference 8. These noise predictions showed an under-prediction of the BVI noise a plane underneath the rotor system and suggested that higher order schemes and/or higher grid densities are needed to improve the predictions. Further examination of the rotor wake system for these same cases in Reference 10 reinforced the need for higher order methods and/or higher grid densities. Based on the above recommendations, Boyd [Ref. 11] further used OVERFLOW2 with a higher order numerical scheme; high grid densities in the regions of expected rotor wake; added the wind tunnel fuselage/sting body; and included elastic blade motions and blade surface pressures in the acoustic code. Results showed improvements in the prediction of rotor loading and BVI noise for a wide range of HHC control phase angles. All subsequent active twist rotor predictions in this study are based on the method and configuration used in Reference 11, with only slight modification to accommodate active twist of the rotor blade as discussed below.

1.2 Active Twist

Unlike HHC, which typically uses swashplate motion to affect rotor blade motion, active twist of the rotor blade uses embedded actuators to affect rotor blade torsional motion. For example, in 2000, a model scale active twist rotor (ATR) [Refs. 12, 13] was tested in the NASA Transonic Dynamics Tunnel (TDT) at the NASA Langley Research Center (LaRC). This was a collaborative effort designed to perform a proof of concept test of an active twist rotor. The primary focus of the testing was vibration reduction; therefore only 3P, 4P, and 5P actuation frequencies were tested. This active twist rotor was built with piezoelectric fiber composite (PFC) actuators embedded in the blade structure and was designed to provide blade torsional control by placing a voltage across the PFC actuators. Results [Ref. 12] from this test showed that the best vibration reductions – in some cases as much as 70 to 95% – were provided by 3P actuation of the PFCs at particular amplitudes and control phase angles. Reference 12 also demonstrated an initial use of the CAMRAD-II comprehensive rotorcraft analysis [Ref. 7] to compare computed vibrations to measured values. Acoustic results [Ref. 13] indicate that (1) BVI noise was most sensitive to 5P actuation, (2) BVI noise reductions of up to 2.8 dB are achievable, but at the cost of higher low frequency noise, and (3) 4P non-rotating vertical hub vibrations could be reduced using 3P actuation, but at the cost of higher low frequency noise. Generally, it was concluded [Ref. 13] that active twist appears to be an effective technique to reduce vibratory loads. Also, comparing the BVI noise reduction per degree of blade pitch or twist, there was little difference between the active twist and the HHC methods.

1.3 Active Twist Prediction Scheme

With the goal of this paper to provide a preliminary examination of a possible subset of active rotor blade twist cases for a potential future rotor test of a HART-II type of configuration, some level of confidence in the predictions is needed when there is no experimental data with which to compare. This confidence is provided by using a method which has previously been successfully applied to the same configuration. The solution method, numerical scheme, rotor/sting configuration, grid densities, etc. are the same here as in Reference 11.

1.4 Active Twist Modeling in CAMRAD-II

Active twist is modeled in CAMRAD-II by applying a periodic torsional moment couple at the root and tip of the blade with the same magnitude, but opposite sign. The magnitude of this applied moment couple is at any azimuth is defined by:

$$M(\psi) = \sum_{n} M_n = \sum_{n} G_n [A_n \cos(n\psi) + B_n \sin(n\psi)]$$

where n is the harmonic number, M_n is the magnitude of the torsional moment couple of the n-th harmonic, G_n is the "gain" of the n-th harmonic, A_n and B_n are the cosine and sine components of the torsional moment couple of the n-th harmonic, and ψ is the azimuth angle. The values of A_n and B_n determine the phase angle, φ_n, of the torsional moment for each harmonic as follows:

$$\varphi_n = \tan^{-1}(B_n / A_n)$$

Using this model, the torsional displacement due to the active twist actuators is not modeled; rather, a torsional moment is applied to affect the torsional displacement. So, at any given phase angle, φ_n , the value of the gain, G_n, can adjusted to obtain the desired elastic torsional response at the tip of the rotor blade.

1.4 Choice of harmonics and amplitudes

In line with the desire to remain "close" to previously predicted results as a means to provide confidence in the active twist predictions, the 3P (n=3) harmonic is the only one examined in the current study. First, the active twist test described above indicates that 3P has the potential to provide the best vibration reduction. Second, this harmonic choice was made because of the success in predicting the measured loading and noise for the 3P HHC results shown in the HART-II cases in Reference 11. As for the choice of the active twist gain, or amplitude, it is noted that the predicted HHC 3P elastic tip deflection amplitude due to 3P HHC was generally between about 1° and 2° in the HART-II cases. So, two values of the gain are used in the CAMRAD-II model such that the active twist control in this study result in 3P elastic rotor blade tip twist values of approximately 1° and 2°, respectively.

2. PREDICTIONS

2.1 Flight Condition

The flight condition used for all cases is the same as that of the HART-II Baseline (BL) case. The shaft is tilted 5.3° aft, the advance ratio is 0.15, the rotor is operated at 1041 RPM, and the thrust coefficient is 0.0044. This is a descent flight condition and is known from to have high BVI noise for this model rotor under the advancing and retreating sides of the rotor. For all cases, the model rotor is trimmed to match a nominal thrust of 3300 Newtons and to null the hub pitch and roll moments by adjusting the collective and 1P cyclic pitch settings; the trim process implicitly includes effects of the active rotor blade twist.

2.2 Loading: Baseline Case

To relate the predictions to previous work and to relate the active twist results to a known quantity, a baseline case ("BL") without active twist inputs is examined at the flight condition discussed. Since this BL case is identical to the HART-II BL case, comparison can be made with measured data. Blade surface pressures in the HART-II effort were measured at the 0.87R radial station. These pressures were then integrated using a piecewise constant pressure assumption to obtain an integrated sectional load [Ref. 2]. This sectional load is then converted to a normal force coefficient multiplied by the Mach number squared (C_NM^2). The predicted surface pressures at 0.87R are also integrated and converted to C_NM^2. In addition to the loading, it is important to examine the time derivative of loading because that quantity has direct importance to the rotor acoustics – especially in the frequencies of interest. The azimuth angle in this case will be used as the "time" variable when computing the "time derivative". Figure 1 shows the measured and predicted C_NM^2 as a function of rotor azimuth (in degrees). It is observed that BVI events are well matched by the prediction method in both number and location. In addition, the temporal derivative shows that the measured BVI events are well match by the predictions.

Boyd [Ref. 11] presents a number of cases that indicate the current prediction method consistently predicts well the changes in BVI aerodynamic events and its associated noise with this rotor system for varying HHC pitch inputs. Subsequent sections show predicted results for this rotor in the same aerodynamic environment, but with active twist of the rotor blades instead of HHC pitch inputs.

2.3 Loading: 3P Active Twist Control Phase Sweep

Figure 2 shows the loading results at 0.87R due to different torsional moment control phase angles. Each figure (that is, each control phase angle) shows results from both the 1° and 2° active twist amplitude predictions. The dominant feature in all of the plots of Figure 2 is the 3P loading due to the 3P active twist torsional motion. It is observed that the BVI events are affected; however, to more clearly see the effects that are related to the noise generated, the temporal derivative of the loading from Figure 2 is presented in Figure 3. Figure 3 shows that the active twist can change the number of, and magnitude of, the BVI events on the advancing side, and, to a lesser amount, the retreating side. Qualitatively, these changes are similar to the changes observed in the 3P HHC phase sweep shown in Reference 11.

2.4 BVI Noise Prediction

The discrete frequency noise is computed with PSU-WOPWOP [Ref. 14] using surface pressures and elastic blade motion for the various torsional moment control phase angles and magnitudes. Figure 4 is provided as a schematic for all subsequent noise contour plots. The circle represents relative location of the rotor disk. The contour represents integrated mid-frequency noise (dB) integrated from 6P to 40P on a microphone plane underneath the rotor. This is identical to the HART-II microphone plane used by Boyd [Ref. 11]. The view is from above the rotor system and the wind tunnel flow direction is indicated.

For the BL case presented in Figure 5, the mid-frequency noise prediction matches well with measured data from the HART-II effort. The BL case shows two high noise regions: one under the advancing side of the rotor and one under the retreating side of the rotor and aft of the rotor center. These high noise levels are indicative of the BVI loading events observed in Figure 1 on the advancing and retreating side of the rotor disk. Figure 6 presents the integrated mid-frequency noise contours for a sequence of active twist control couple phase angles. Several global features can be noted. First, as expected, the higher amplitude inputs produce larger changes to the noise directivity than the lower amplitude inputs. Also, by comparing these changes to the directivity changes due to 3P HHC seen in Reference 11, it is observed that the changes due to the higher amplitude active twist inputs are similar qualitatively – and in some cases, quantitatively – to the 3P HHC results. Figure 6, however, shows that higher amplitude of active twist input is required to attain the same level of BVI noise change as that from the HHC approach. This is consistent with findings of Booth, et al [Ref. 13] where it was concluded that, when using similar active twist and HHC inputs, the active twist inputs were less effective in reducing BVI noise.

To more clearly observe the changes associated with the active twist inputs, Figure 7 presents the change in maximum BVI noise level (relative to the predicted HART-II baseline level) extracted from the data contained in Figure 6. The horizontal axis is the control phase angle of the active twist input and the vertical axis is the dB level change. Consistent with HHC phase angle sweeps in Reference 11, the maximum BVI noise level increases and decreases with active twist control phase angle. The trend with both active twist amplitudes is similar in general, and the predictions show the best noise reduction potential for control phase angles between about 60° and 120°. The maximum reduction in noise is approximately 3.3 dB at the 2° amplitude at a control phase angle of about 120°.

2.5 Vibration

Active twist has also been explored as a means to potentially reduce hub vibrations [Ref. 12] Figure 8 presents the sine component versus the cosine component of the fixed system 4P vertical hub shear. The figure is presented in a manner similar to Reference 12. The open diamond symbol represents the HART-II baseline case. For each active twist control amplitude, a line identifies the location of the case for which the active twist control phase is 0°. Control phase angles increase in increments of 60° from this line in a counter-clockwise direction. It is observed that the 1° amplitude case forms (approximately) a circle surrounding the baseline case. However, this circle does not include the plot origin, which would indicate the ability to eliminate the 4P vibratory component of the load. However, the 2° amplitude active twist cases do form a circle that encompasses the origin. Based on these two results, it appears that for this flight condition and this rotor, an active twist input with an amplitude of approximately 1.5° at a phase angle of approximately 90° could have the potential to nearly eliminate this vibratory component. The control phase angle range for predicted vibration reduction potential is predicted to overlap the control phase angle range for predicted noise reduction. Therefore, the predictions indicate a potential to achieve reduction in both simultaneously.

This type of analysis can be performed for any similar quantity of interest (i.e., other 4P hub forces, 4P hub moments, 8P forces and moments, etc), but a thorough evaluation is beyond the scope of this study.

2.6 Performance

The predicted results above indicate that, for this particular flight condition and rotor system, a modest (~3dB) mid-frequency noise reduction is possible while also reducing the 4P vertical non-rotating hub load. However, the performance of the rotor must also be examined to determine if the decrease in noise and/or vibration is accompanied by a significant performance penalty. The performance impact is briefly assessed here by examining the changes the rotor lift-to-drag ratio. Figure 9 shows the percent change in the rotor lift-to-drag (L/D) with respect to the BL case. With the exception of one control phase angle for one amplitude, all cases show between a 1.2% to 5.5% decrease in the rotor L/D for the 1° active twist amplitude inputs and nearly a 15% decrease for the 2° inputs. For the HHC cases in Reference 11, the same L/D “penalty” falls within the same range as the 1° active twist amplitude above.

Examination of the power quantities in CAMRAD-II for the active twist cases indicates that, for all but the one “exception case” above, the profile power is higher than the baseline case. Because profile power is computed from a radial integration of the sectional drag, this is an indication that the 3P active twist inputs cause the rotor drag to increase, resulting in the overall lower rotor L/D ratio. So, for the cases examined here, it seems clear that the predictions indicate there is potentially a performance penalty for the modest noise reduction and decreased vibration of this particular active twist. However, it should be noted that this is only a preliminary study of just one particular aspect of active twist usage.

3. SUMMARY

For a descent flight condition at an advance ratio of 0.15 and an aft shaft tilt of 5.3°, a loosely coupled CFD/CSD/Acoustic method was used to predict the effects of active twist on loading, mid-frequency noise, vibration, and performance for a rotor and fuselage/sting geometry identical to the previously studied HART-II system. Whereas previous predictions used the HART-II 3P HHC cases, the current method applies a periodic torsional moment couple at the root and tip of the blades to produce active twist of the entire rotor blade at a given frequency and amplitude. An active twist harmonic and amplitude was chosen to result 3P tip torsional motion similar to that seen in previous successful predictions. This provides a high level of confidence in the predicted results when there is no experimental data with which to compare for this particular rotor system. Two active twist amplitudes were examined at a range of control phase angles. This a full sweep of active twist control phase angles for the 3P input shows that:

- The advancing side BVI loading events indicated in the $C_N M^2$ and $dC_N M^2/d\psi$ loading are affected by various phase angles. The retreating side BVI loading events are also affected, but not as strongly as the advancing side events. The higher amplitude active twist inputs had a more dramatic effect than the lower amplitude inputs.

- The mid-frequency noise directivity patterns for the higher amplitude of active twist input resulted in qualitatively and quantitatively similar results to similar HART-II HHC cases that had an equivalent of 0.8° of 3P pitch at the pitch bearing (but, had 3P elastic tip twist similar to the active twist cases).

- For this particular flight condition and rotor configuration, it was shown that using 3P active twist, there is a potential to both reduce the 4P vertical hub non-rotating forces and to reduce BVI noise simultaneously using an active twist amplitude of approximately 1.5° for a select range of control phase angles.

- Though a subset of the cases examined indicate a potential to reduced noise and vibration, nearly all cases suffer from a reduction of rotor L/D due to increase blade sectional drag, as indicated by increases in the rotor profile power component. Comparison between the predictions of the L/D reduction for the HHC cases and the active twist cases indicate that the 1° amplitude active twist has about the same L/D reduction as the HHC cases, but the 2° amplitude active twist inputs dramatically increase the L/D reduction.

4. ACKNOWLEDGEMENTS

The author would like to thank Matt Wilbur (U.S. Army Research Labs) and Dr. David Fogarty (National Institute of Aerospace) for discussion and assistance in modeling active twist with CAMRAD-II.

5. REFERENCES

1 Yu, Y.H., Gmelin, B., Splettstoesser, W., Philippe, J.J., Prieur, J., Brooks, T.F., "Reduction of Helicopter Blade-Vortex Interaction Noise by Active Rotor Control Technology", Progress in Aerospace Science, Vol. 33, pp 647-687, 1997.

2 van der Wall, B.G., Burley, C.L.: "2nd HHC Aeroacoustic Rotor Test (HART-II) – Part II: Representative Results", German Aerospace Center Institute Report IB 111-2005/03, February 5, 2005.

3 Brooks, T.F., Boyd, Jr., D.D., Burley, C.L., Jolly, Jr., R.J., "Aeroacoustic Codes for Rotor Harmonic and BVI Noise – CAMRAD.Mod1/HIRES", Journal of the American Helicopter Society, Vol 45, No. 63, April 2000.

4 Burley, C.L., Brooks, T.F., Marcolini, M. A., Brand, A.G., Conner, D.A.: Tiltrotor Aeroacoustic Code (TRAC) Predictions and Comparison with Measurements", Journal of the American Helicopter Society, Vol 45, No. 80, April 2000.

5 Boyd, Jr., D.D., Burley, C.L., Conner, D.A.: "Acoustic Predictions for Manned and Unmanned Rotorcraft Using the Comprehensive Analytical Rotorcraft Model for Acoustics (CARMA) Code System", American Helicopter Society International Specialists' Meeting on Unmanned Rotorcraft, Jan 18-20, 2005, Phoenix, Arizona.

6 Nichols, R.H., Tramel, R.W., Buning, P.G.: "Solver and Turbulence Model Upgrades to OVERFLOW2 for Unsteady and High-Speed Applications", AIAA Paper 2006-2824, June 2006.

7 Johnson, W.J.: "CAMRAD-II: Comprehensive Analytical Model for Rotorcraft Aerodynamics and Dynamics", Volumes 1-9, Johnson Aeronautics, Palo Alto, CA, 2007.

8 Lim, J.W., Nygaard, T.A., Strawn, R., Potsdam, M.: "BVI Airloads Prediction using CFD/CSD Loose Coupling", American Helicopter Society

Fourth Vertical Lift Aircraft Design Conference, San Francisco, California, January 18-20, 2006.

9 Sim, B.W., Lim, J.W.: "Blade-Vortex Interaction (BVI) Noise & Airload Prediction using Loose Aerodynamic/Structural Coupling", 62nd American Helicopter Society Forum, Phoenix, Arizona, May 2006.

10 Lim, J.W., Strawn, R.: "Prediction of HART-II Rotor BVI Loading and Wake System using CFD/CSD Loose Coupling", Journal of Aircraft, Vol. 45, No. 3, May-June 2008.

11 Boyd, Jr., D.D.: "HART-II Acoustic Predictions using a Coupled CFD/CSD Method", 65th American Helicopter Society Forum, Grapevine, Texas, May 27-29, 2009.

12 Wilbur, M.L., Yeager, Jr., W.T., Sekula, M.K.: "Further Examination of the Vibratory Loads Prediction Results from the NASA/Army/MIT Active Twist Rotor Test", 58th American Helicopter Society Forum, Montréal, Canada, June 11-13, 2002.

13 Booth, E.R., Wilbur, M.L.: "Acoustic Aspects of Active-Twist Rotor Control", 58th American Helicopter Society Forum, Montréal, Canada, June 11-13, 2002.

14 Brentner, K.S., Perez, G., Brès, G.A., Jones, H.E.: "Toward a Better Understanding of Maneuvering Rotorcraft Noise," American Helicopter Society 58th Annual Forum, Montréal, Canada, June 11-13, 2002.

6. FIGURES

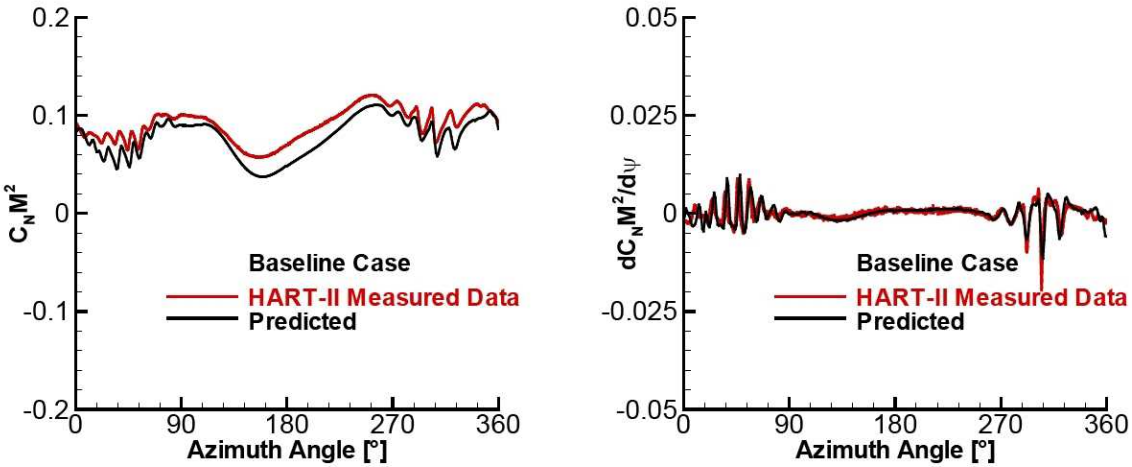

Figure 1: Measured and predicted $C_N M^2$ and $dC_N M^2/d\psi$ for the HART-II Baseline case.

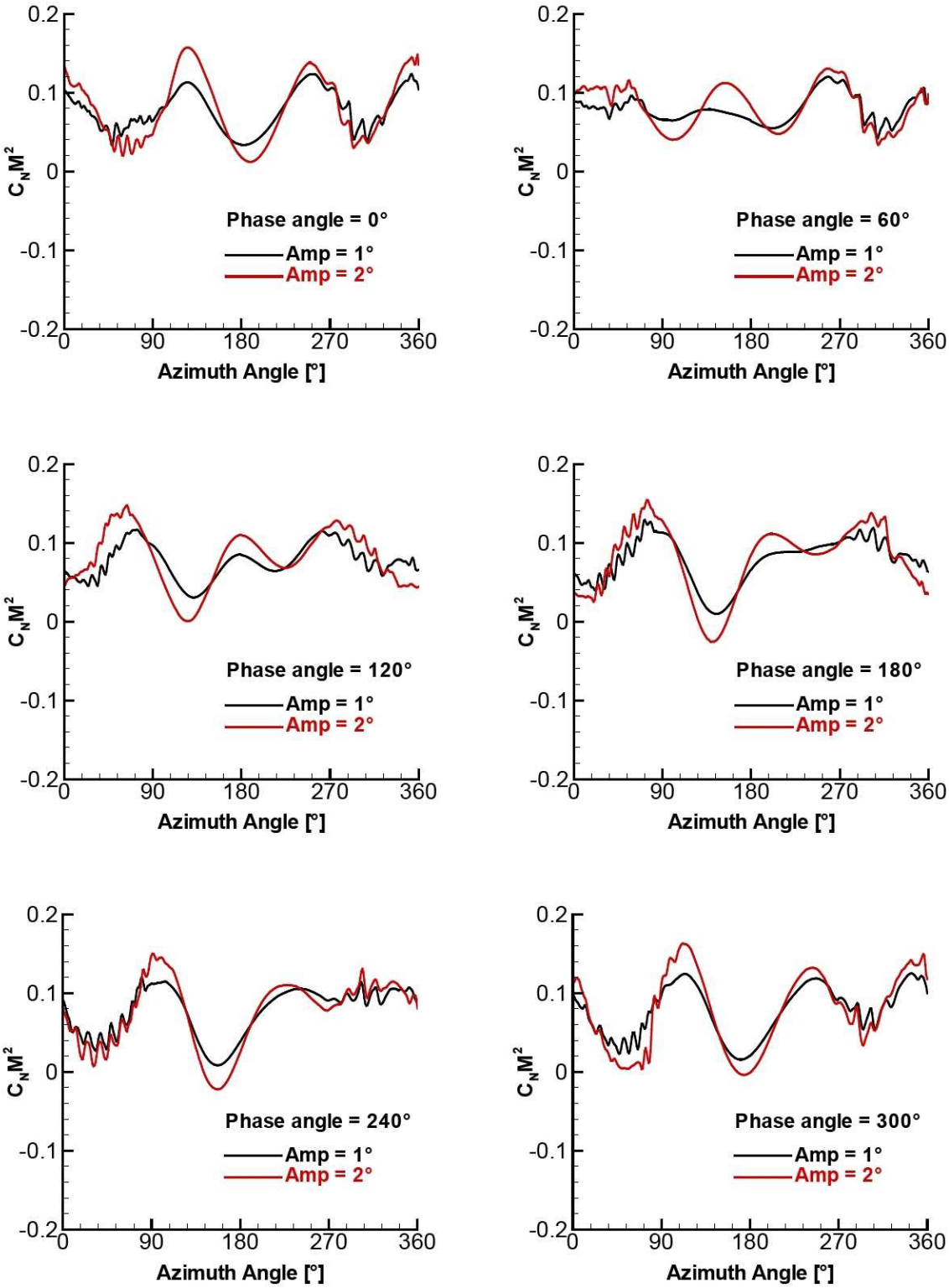

Figure 2: Predicted Loading at r=0.87R for 3P active twist amplitudes of 1 and 2 degrees.

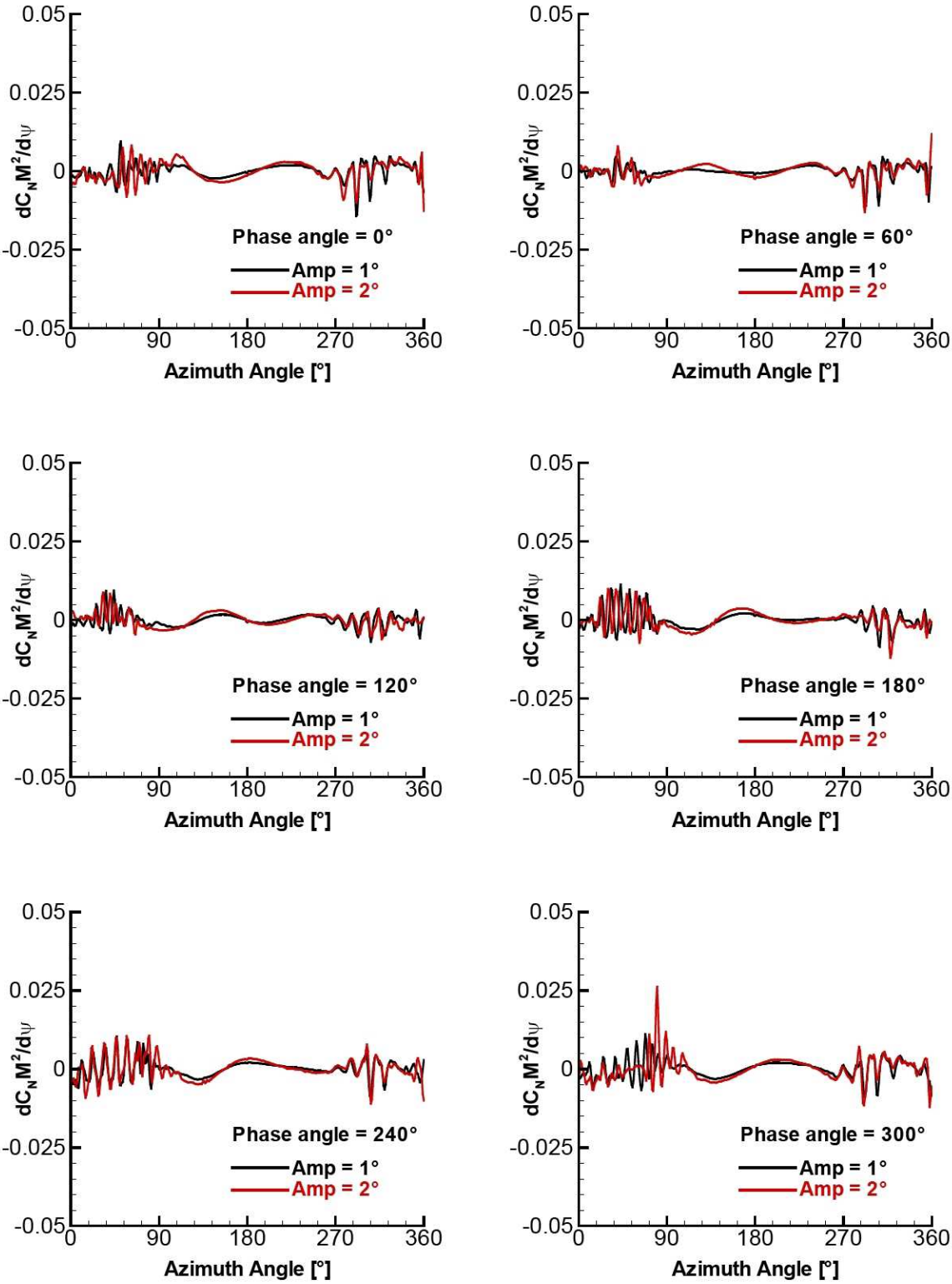

Figure 3: Predicted Loading derivative at r=0.87R for 3P active twist amplitudes of 1 and 2 degrees.

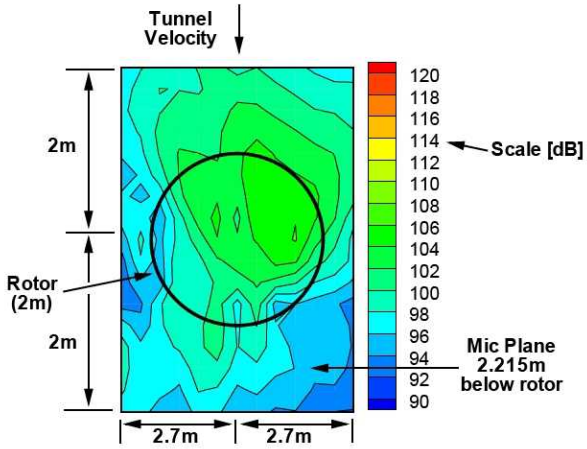

Figure 4: Schematic describing all noise contour maps in the following figures.

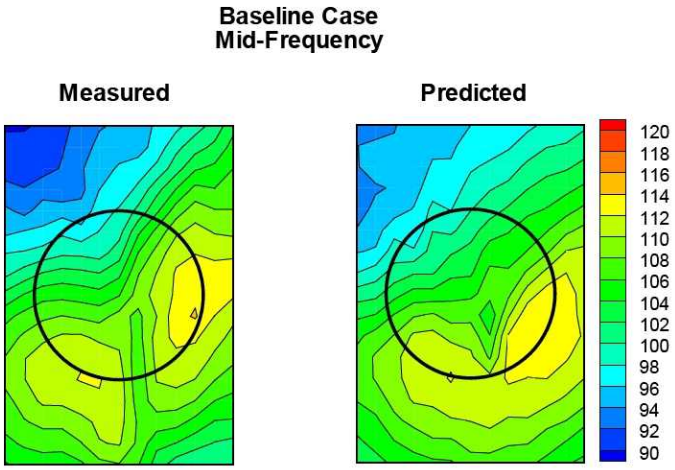

Figure 5: Mid-Frequency noise: HART-II measured data from BL case vs. prediction.

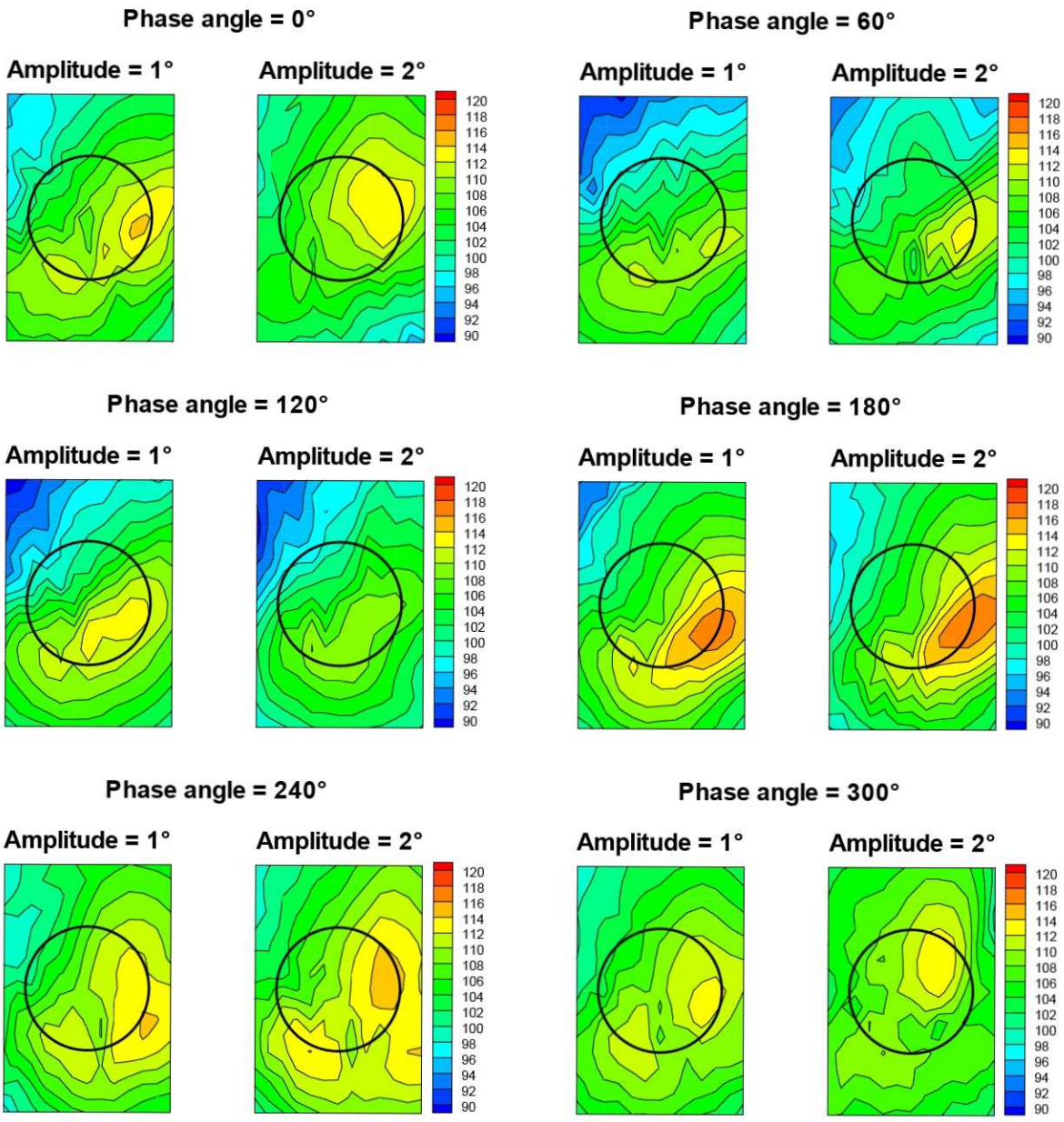

Figure 6: Predicted Mid-Frequency noise contours on a plane under the rotor for a phase angle sweep at 1 and 2 degrees amplitude.

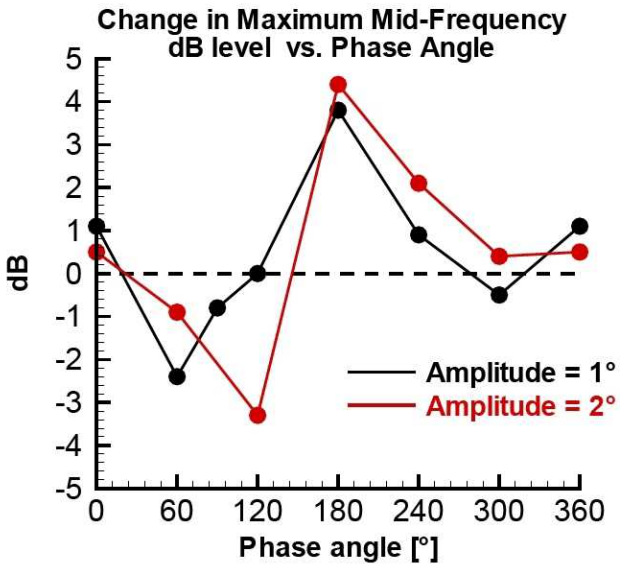

Figure 7: Change in maximum BVI noise level (relative to the predicted HART-II baseline case in Figure 5) as a function of active twist phase angle.

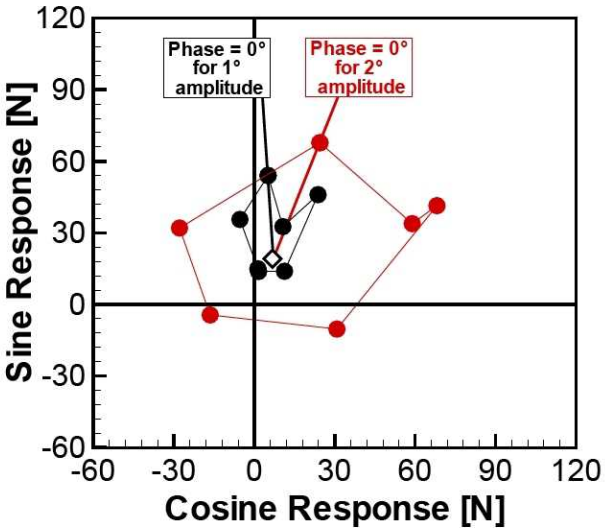

Figure 8: Predicted sine and cosine components of the 4P non-rotating hub vertical force (along the shaft axis). Open diamond symbol is the HART-II baseline case. Black and red circles are the 1° and 2°amplitudes, respectively. The 0° phase angle line is identified for each amplitude and phase angles increase counter-clockwise from this line.

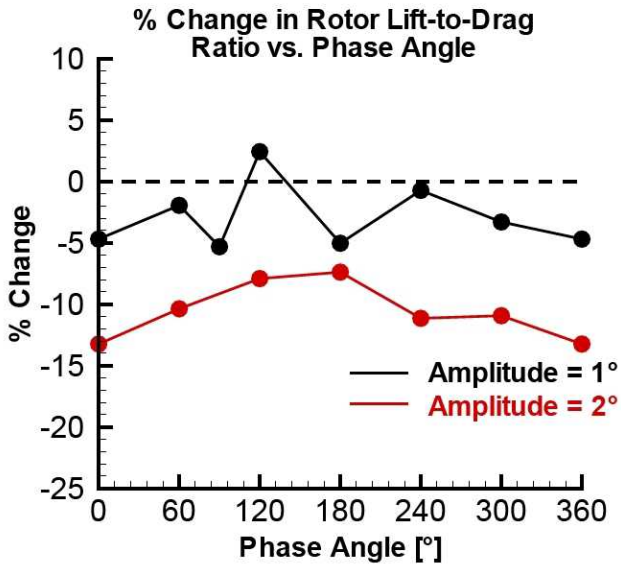

Figure 9: Percent change in rotor lift-to-drag ratio for a range of torsional moment phase angles.